Semi-Automatic Identification of Optic Disk by Image Processing for Quantitative Funduscopy

WILIAN FLÁVIO RIGO [1] AURELIO PAULO BATISTA DA SILVA [2], THOMAS WALTER RAUBER [3]

[1,3]UFES–Universidade Federal do Espírito Santo - Departamento de Informática, Centro Tecnológico
{wilian,thomas}@inf.ufes.br
[2]UFES–Universidade Federal do Espírito Santo - Departamento de Morfologia, Centro Biomédico
apbatista@escelsa.com.br

Abstract. This paper describes the current state of research and development of a system for the partial automation of quantitative Funduscopy. Image processing techniques are used to segment the optic disk and estimate the parameters of the circumference associated with it. The global objective is to facilitate the diagnosis of pathologies like Systemic Arterial Hypertension and Diabetes Mellitus.

1 INTRODUCTION

The examination of the back part of the eyeball (fundus) aka. ophthalmoscopy or funduscopy has as its objective the study of the retina as well as the providing blood vessels (arteries and veins). The transparent structures that compose the eyeball permit that the microvascularity of the retina can be observed by relatively simple optical equipment. A typical image of the retina acquired by a ophthalmoscope is shown in figure 1. Illnesses like Diabetes Mellitus, Systemic Arterial Hypertension, glaucoma and optic nerve damage potentially provoke modifications which can lead to irreversible damage to vision if not treated in time. Since the fundus is the only part of the human body where one can observe blood vessels by non-invasive means, funduscopy provides a methodology to examine and evaluate the state of the blood vessels by simple observation.

Currently funduscopy is executed manually in a qualitative manner. Diagnostics are issued by directly observing the fundus of the patients eyeball. This qualitative analysis gives rise to many variations in the interpretation of the observed symptoms causing consequent variations of the diagnostics due to the dependency on the different experience of the professional that realizes the examination and on the used ophthalmoscope. Individuals at an advanced age can present symptoms of Retinal Hypertension (RH) without actually having the illness because the alterations can naturally occur with elder people. Hayreh et al. [4] comment the discords in the interpretation of the relation of the vascular diameter between arteries and veins in conventional ophthalmoscopy, both intra-observer and inter-observer like, thus characterizing this criterion to be interpreted with great difficulty. Dimmitt and co-workers [1] quantify the inter-observer variation as 38%, regarding fundus abnormalities diagnosed by direct ophthalmoscopy. Lenders [6] mentions further conditions which limit ophthalmoscopy, like the duration spend for the examination, the necessity of an experienced observer and the fact being a qualitative evaluation.

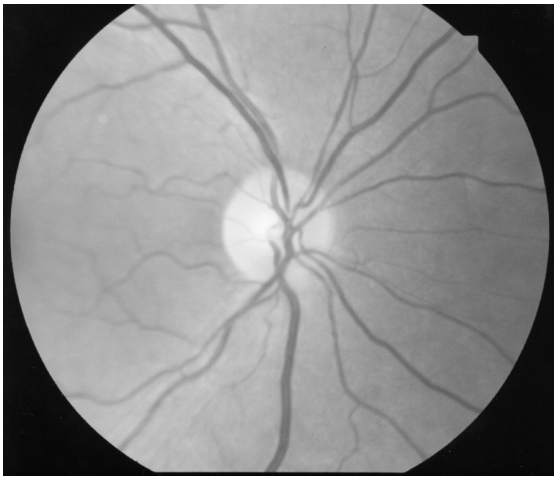

Figure 1: Image of the retina. The brighter central region forms the optic disk where the blood vessels converge.

Recently quantitative methodologies to investigate the vascularity of the retina have been employed thus diminishing the variation of the diagnosis among the professionals. Statistical studies show that manual examinations present a variation between 6% and 34%, whereas semi-automatic techniques reduce this variation to between 1,5% and 7,5%. Motivated by the difficulties the diameter of the vessels, Newsom et al. [7] compare the measure of the vascular diameter obtained by an observer to a computerized method. They observe that in conventional ophthalmoscopy the blood columns were larger compared to the automated diagnosis characterizing a methodological error of the examiner.

The objective of this work is to develop and refine a tool that is less sensible and specific, able to automate the quantitative methodology for the examination of the fundus thus reducing the intrinsic errors of the qualitative techniques. In this first stage of the work we concentrate on the determination of the optic disk. The idea is to limit

the subjective influence of the professional when it comes to the delineation of the brighter area of the fundus that constitutes the disk. By forcing a quantitative analysis to accept the segmentation of the disk by a semi-automatic image processing software, subsequent phases of analyses that use the optic disk as a reference are less sensible to subjective errors. The ability to reproduce the analysis is a significant advantage of our proposal since the result of the segmentation depends on the employed algorithms and their fixed parameters. Relevant work regarding image processing for the detection of the optic disk are for instance [5] which try to determine the disk by pyramidal decomposition and Hausdorff-based template matching. Huiqi and Chutatape [**?**] try to fully automate the detection by using clustering the brightest pixels in the intensity image, applying Principal Component Analysis and distance measure in the projected space to determine the center. An interesting approach using deformable models (snakes) to the contour delineation problem was applied by Mendels et al. [**?**]. The Hough transform was used by [**?**] to estimate the optical disk. The paper is organized as follows. In chapter 2 we describe the image processing techniques used to determine the optic disk, in chapter 3 we provide the results of the theoretical bases applied to real images of the retina and finally in chapter 4 we expose the limitations of the method and give an outlook for further research.

2 Optic Disc Segmentation

We divide the task to determine the area of the optic disk into independent image processing and optimization modules. In the first pass we apply a normalization to the pixel intensities in order to compensate for eventual artifacts introduced by the image acquisition hardware. With the equipment used, usually a global gradient of the pixel intensities can be observed along a linear direction of the image which must be compensated for. The second pass comprises of a semi-automatic segmentation step in which the operator indicates a pixel that belongs to the optic disk. A region-growing algorithm is used to obtain a part of the disk area. In the third part a Backtracking Bug Follower Algorithm is used to obtain the contour of this disk fragment. Finally in the last pass again in a semi-interactive way a segment of the contour is indicated which constitutes a partial arc of the circumference associated to the disk. An optimization algorithm is used to estimate the three determining parameters of the disk, x and y coordinates of the center and radius.

2.1 Normalization

In the experiments that we performed the image acquisition was done by acquiring a optical photograph using a 35 mm camera coupled to a Nikon NF505 ophthalmoscope. A global gradient of the pixel intensities can be observed in all of the images used. This means that a homogeneous area of the retina seems darker or brighter if observed along a line of the acquired $N \times M$ image. Considering the intensities $f^{(b)}(i,j)$ of the pixels at positions $0 \leq i \leq N-1$, $0 \leq j \leq M-1$ independently for each band b of the RGB model, $b \in \{r,g,b\}$ we calculate a new intensity $f^{(b)}_{\text{new}}(i,j)$ as

$$f^{(b)}_{\text{new}}(i,j) = f^{(b)}_{\text{old}}(i,j) * \overline{m}^{(b)}/m^{(b)}_i \qquad (1)$$

where $m^{(b)}_i = \text{med}\{f^{(b)}(i,j)\}$, $j = 0 \ldots M-1$ is median value of the pixels of the i-th line and $\overline{m}^{(b)}$ is the mean of all $m^{(b)}_i$, $i = 0 \ldots N-1$.

In a second pass the whole procedure is repeated along the columns thus eliminating problems of rotation sensitive line-based compensation procedure.

For each line of the image the median is calculated in order to disregard the influence of intensities that deviate too much from the mean. This choice has the effect that neither darker areas like blood vessels nor brighter areas like the optic disk influence the mean value of each line too much. The resulting vector $\mathbf{m}^{(b)}$ usually shows the global gradient artifact of the acquisition process.

The effect of this first preprocessing step is that the image is globally more homogeneous along a certain direction. A positive effect related to this property is that the following region-growing segmentation algorithm deals with regions that do not present artificial differences at the extremes of the region which would degenerate the contour of the segmented region. The image is now prepared for the next stage which is the partial segmentation of the optic disk.

2.2 Segmentation

Stanton et al. [9] characterize a region of interest in the fundus image defined by the circular optic disk and another circumference with a radius four times larger than that of the central optic disk but with the same center. Hence our goal is to outline the inner circumference or at least a part of it. The ideal optimal segmentation of the total disk area for instance by simple histogram based segmentation is virtually impossible since the vessels converge in the central area and due to their different brightness relative to the disk fundus do not allow to obtain a contiguous region.

The semi-automatic algorithm requires three parameters from the operator: an initial point belonging to the disk area to be segmented, a number of *barrier* pixels and a percentage of tolerance of deviation from the initial point. The initial pixel $\mathbf{p}(i,j)$ is visually specified by the operator using a locator device (e.g. a mouse). This methodology ensures that erroneous initial conditions of the segmentation

procedure are excluded since the initial point is a part of the optical disk.

The algorithm works in the usual region-based expansion [3] recursively analyzing the 4-neighbors of each pixel until the segmentation criterion is not satisfied anymore for all candidate pixels. We define the *tonality* $v(i,j)$ of the pixel at position (i,j) as the heuristic $f^{(g)}(i,j) + f^{(b)}(i,j)$. The red band is omitted in this criterion since it carries a negligible amount of information. The deviation tolerance T specified by the operator finally defines the segmentation criterion. If the tonality $v(i^{'}, j^{'})$ of all barrier pixels falls below the permitted tolerance then the partial segmentation is terminated, i.e. if

$$v(i^{'}, j^{'}) \leq v(i,j)(1-T). \tag{2}$$

Starting from a pixel at position (i,j), the region expansion algorithm searches a number of B consecutive pixels either in a horizontal or vertical sequence. If all these B barrier pixels satisfy the segmentation criterion 2 then (i,j) belongs to the region. For instance searching toward east all pixels $(i, j+1), \ldots, (i, j+B)$ satisfy 2.

The result of this processing module is a contiguous region that delimits a part of the optical disk, including a partial arc of the boundary of the disk which is essential for the next phase.

2.3 Contour Detection of Partial Optic Disc

As mentioned before the goal of this processing module is to obtain those coordinates which delimit the contour of the area segmented by the region growing algorithm. This is a well studied task in image processing since there is no uncertainty involved in the process. The Backtracking Bug Following algorithm described by Pratt [8] starts with an initial contour point and simulating the movements of an insect orienting itself along the border finds the next contour pixel until reaching the initial position.

Due to the imperfect segmentation of the region growing algorithm, the contour tracker finds a border that can be divided into two principal parts. The first is a contiguous sequence of pixels that truly lie on the border of the optic disk. The second part are pixels which belong to the interior region of the disk. Once again the interaction of a human operator is required to specify two points belonging to the border. The algorithm then collects N points $X = \{(x_i, y_i)\}_{i=1}^{N}$ between which all belong to the border of the optic disk.

2.4 Parameter Estimation of Optic Disk

The point set X determined will finally serve as the data samples of a nonlinear optimization algorithm for circle fitting with the objective to determine the three describing parameters of a circumference, $\mathbf{u} = (C_x, C_y, R)^T$, the coordinates of center $\mathbf{C} = (C_x, C_y)$ and the radius R. We follow the method proposed by Gander et al. [2]. In a first pass an initial guess of the parameter vector $\mathbf{u}^{(0)}$ can be obtained by a linear solution by minimizing the algebraic distance between the points and the model.

We define the mean square distance between the data points and the analytical parameters that define the circle as

$$E(\mathbf{u}) = \sum_{i=1}^{N} [(x_i - C_x)^2 + (y_i - C_y)^2 - R^2]^2 \tag{3}$$

The parameters $\mathbf{u}_{\min}$ that minimize this distance satisfy $\nabla E(\mathbf{u}) = \mathbf{0}|_{\mathbf{u}=\mathbf{u}_{\min}}$, i.e. $\partial E/\partial C_x = 0$, $\partial E/\partial C_y = 0$ and $\partial E/\partial R = 0$. These constraints define a linear system

$$\mathbf{X}\mathbf{w} = \mathbf{t} \tag{4}$$

where $\mathbf{X}$ is a $N \times 3$ matrix where each line contains the ith augmented data point $[x_i \; y_i \; 1]$, $\mathbf{w}$ is a coefficient vector of the form $\mathbf{w} = [a \; b \; c]^T$, $a = -2C_x$, $b = -2C_y$, $c = C_x^2 + C_y^2 - R^2$, from which the desired parameter vector $\mathbf{u}$ (more specifically the initial guess $\mathbf{u}^{(0)}$) can be derived and $\mathbf{t}$ is a N-dimensional vector of expressions $[-x_i^2 - y_i^2]$.

The initial coefficients can directly be calculated by the Moore-Penrose Pseudoiverse matrix $X^{\dagger} \equiv (\mathbf{X}^T\mathbf{X})^{-1}\mathbf{X}^T$ as

$$\mathbf{w}^{(0)} = X^{\dagger}\mathbf{t} \tag{5}$$

and finally the initial guess $\mathbf{u}^{(0)}$ using the relation between $\mathbf{u}$ and $\mathbf{w}$

$$\begin{aligned} u_1 &= C_x = -a/2 \\ u_2 &= C_y = -b/2 \\ u_3 &= R = \sqrt{C_x)^2 + C_y)^2 - c}. \end{aligned} \tag{6}$$

As mentioned earlier [2] the algebraic solution to the mean square distance minimization problem is often not satisfactory enough. In order to minimize the geometric distance $d(\mathbf{u})$ with

$$\begin{aligned} d_i(\mathbf{u}) &= \left\| \begin{pmatrix} C_x \\ C_y \end{pmatrix} - \begin{pmatrix} x_i \\ y_i \end{pmatrix} \right\| - R \\ d(\mathbf{u}) &= \sum_{i=1}^{N} [d_i(\mathbf{u})]^2 \end{aligned} \tag{7}$$

Using Gauss-Newton optimization we can formulate the l-th iteration as the linear system

$$\mathbf{J}(\mathbf{u})\mathbf{h} = -\mathbf{F}(\mathbf{u}) \tag{8}$$

where $\mathbf{J}(\mathbf{u})$ is the $N \times 3$ Jacobian consisting of elements $(J)_{ij} = \partial d_i(\mathbf{u})/\partial u_j$, $\mathbf{h}$ is a 3-dimensional residual vector

ideally converging toward $\mathbf{0}$ and $\mathbf{F}(\mathbf{u})$ is a N-dimensional vector with elements $(\sqrt{(C_x - x_i)^2 + (C_y - y_i)^2} - R)$. In the concrete case $\mathbf{u} = (C_x, C_y, R)^T$, one line of the Jacobian is given by

$$\left(\frac{C_x - x_i}{\sqrt{(C_x - x_i)^2 + (C_y - y_i)^2}} \quad \frac{C_y - y_i}{\sqrt{(C_x - x_i)^2 + (C_y - y_i)^2}} \quad -1 \right).$$

The residual vector $\mathbf{h}$ can once again be obtained using the Pseudoinverse $\mathbf{J}^\dagger(\mathbf{u}) \equiv (\mathbf{J}^T\mathbf{J})^{-1}\mathbf{J}^T$ as

$$\mathbf{h} = \mathbf{J}^\dagger(\mathbf{u})(-\mathbf{F}(\mathbf{u})). \tag{9}$$

Finally the new values of the desired coefficient vector is updated in the next iteration as

$$\mathbf{u}^{(l+1)} := \mathbf{u}^{(l)} + \mathbf{h}. \tag{10}$$

The recursive estimation of $\mathbf{u}$ is stopped if $\|\mathbf{h}\|$ falls below a predefined threshold.

Resuming on determining of the parameters center and radius of the optic disk we first provide an initial guess $\mathbf{u}^{(0)}$ by (5) and (6) then at each iteration step the Jacobian and function $\mathbf{F}$ are calculated, the residual is determined by (9) and $\mathbf{u}$ is updated by (10).

3 Results

We present preliminary results to prove the usefulness of our approach for the detection of the optic disk. One of the drawbacks related to the experiments below is the lack of statistical significance. It is extremely difficult to obtain a sufficiently large database of fundus images to corroborate the theoretical proposals. Nevertheless we claim that the visually inspectable results are quite encouraging since the optic disk is delimited in a manner similar to that of a human being.

3.1 Normalization

In our particular acquisition environment the image is surrounded by a dark area resulting from the difference between the circular image and the rectangular background, see figure 1. The dark pixels must be excluded a priori from any subsequent processing steps. Therefore a fixed threshold of band specific RGB values was established as $(120, 80, 60)$ below which the pixel is excluded from the calculus of the normalization value. Figure 2 justifies the choice of the median of each line (or column) comparing it to the mean, showing that the median is less sensitive to local intensity changes than the mean. Figure 3 shows the normalized version of figure 1.

3.2 Segmentation and Contour Detection of Partial Optic Disc

For the experiments employed, the number of barrier pixels was set to $B = 10$, the deviation tolerance was fixed at

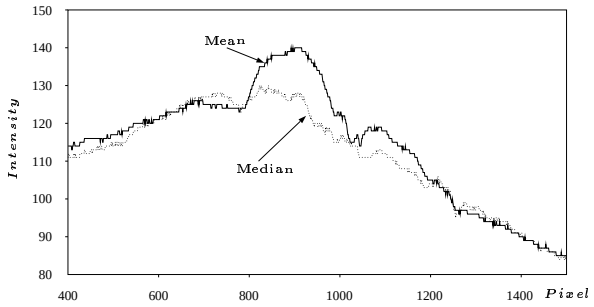

Figure 2: Comparison between the median and mean for intensity normalization. The image shows the intensities of the b-band of the columns between line 400 and 1500 of the image of figure 1. The peak of the mean at about 900 is due to the optic disk.

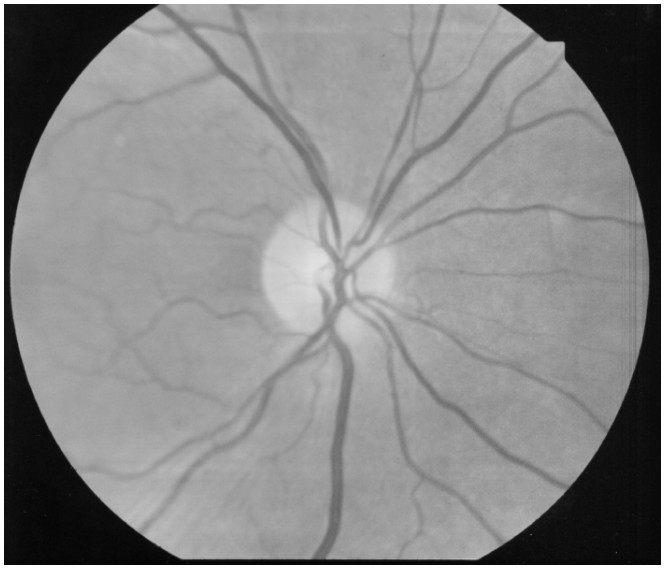

Figure 3: Retina image of figure 1 after normalization.

$T = 23$. The segmentation result of the partial region of the disk is presented in figure 4.

Figure 4: Partial region of the optic disk used to obtain a partial arc of the contour.

The Backtracking Bug Follower determines the contour of the partial region (highlighted in figure 4) which contains the partial arc of the disk which interests us. The operator is required to deliver two coordinates that lie on the contour of disk, marked with a cross in figure 4. Note that the choice of the two points does not influence the determination of the complete contour to a large extent since the subsequent optimization algorithm is robust in terms of the number of arc pixels delivered.

3.3 Parameter Estimation of Optic Disk

The final step is applied to the pixels that constitute the partial arc. The initial guess calculated from (5) and (6) is $C_x^{(0)} = 821.63$, $C_y^{(0)} = 1002.44$ and $R^{(0)} = 209.17$. We stop the updating of the parameters $\mathbf{u}$ by (10) if the norm of residual vector $\|\mathbf{h}\|$ falls below 10^{-4}. The evolution of the residual vector $\mathbf{h}$ of (9) can be observed from table 1. The final values after 3 iteration steps was $C_x^{(XXX)} = 821.73$, $C_y^{(XXX)} = 1003.127$ and $R^{(XXX)} = 209.77$.

4 Conclusions and Future Work

In this paper we have presented a prototype for the semi-automatic determination of optic disk in funduscopy. With the help of image processing and optimization techniques we try to provide a framework which helps a specialist to have a reproducible tool which aids in the calibrated determination of the extension of the optic disk. It could serve as a basis for further diagnostic procedures which take the outline of the disk as a reference.

Step	*Residual* $\mathbf{h}^T$	$\|\mathbf{h}\|$
1	$\begin{pmatrix} 0.092752 & 0.677479 & 0.597575 \end{pmatrix}$	0.908118
1	$\begin{pmatrix} -0.001723 & 0.003369 & 0.002847 \end{pmatrix}$	0.004735
1	$\begin{pmatrix} -0.000023 & 0.000078 & 0.000041 \end{pmatrix}$	0.000091

Table 1: Evolution of the residual vector $\mathbf{h}$ of (9) using Gauss-Newton optimization to improve the circle parameters.

As mentioned earlier we would like to have more data at our disposition to be able to provide statistical evidence about the viability of the proposed methodology. We will try to apply the system to a larger number of benchmark images.

References

[1] S. B. Dimmitt, S. M. Eames, P. Gosling, J. N. W. West, J. M. Gibson, and W. A. Littler. Usefullness of ophthalmoscopy in mild to moderate hypertension. *Lancet.*, pages 1103–1105, 1989.

[2] W. Gander, G. H. Golub, and R. Strebel. Least-squares fitting of circles and ellipses. *BIT*, 43:558–578, 1994.

[3] R. C. Gonzalez and R. E. Woods. *Digital Image Processing*. Addison-Wesley, Reading, MA, USA, 3rd edition, 1992.

[4] S. S. Hayreh, G. E. Servais, and P. S. Virdi. Retinal arteriolar changes in malignant arterial hypertension. *Ophthalmologica.*, (198):178–196, 1989.

[5] M. Lalonde, M. Beaulieu, and L. Gagnon. Fast and robust optic disc detection using pyramidal decomposition and hausdorff-based template matching. *IEEE Transactions on Medical Imaging*, 20(11):1193–1200, 2001.

[6] J. W. M. Lenders. Hypertension and target organ damage. *Netherlands journal of medicine.*, (47):141–144, 1995.

[7] R. S. B. Newsom, P. M. Sullivan, M. B. Rassam, R. Jagoe, and E. M. Kohner. Retinal vessel measurement: Comparison between observer and computer driven methods. *Graefe's Arch Clin Exp Ophthalmol.*, (230):221–225, 1992.

[8] W.K. Pratt. *Digital Image Processing.* Wiley-Interscience Publication., New York, 1991.

[9] A. V. Stanton, P. Mullaney, F. Mee, E. T. O'Brien, and K. O'Malley. A method of quantifying retinal microvascular alterations associated with blood pressure and age. *Journal of Hipertension.*, (13):41–48, 1995.